Manuscript for Genes to Cells

Deficiency of the basic helix-loop-helix transcription factor DEC1 prevents obesity induced by a high-fat diet in mice

Mitsuhide Noshiro[1], Takeshi Kawamoto[1,2*], Ayumu Nakashima[3], Noritsugu Ozaki[1], Toshinori Ueno[3], Masayumi Saeki[4], Kiyomasa Honda[1], Katsumi Fujimoto[1], and Yukio Kato[1]

[1]From Department of Dental and Medical Biochemistry, Institute of Biomedical and Health Sciences, Hiroshima University, Hiroshima, Japan

[2]Writing Center, Hiroshima University, Higashi-Hiroshima, Japan

[3]Department of Nephrology, Hiroshima University Hospital, Hiroshima, Japan

[4]Health Examination Center, Chugoku Rousai Hospital, Kure, Japan

[*]Correspondence: tkawamo@hiroshima-u.ac.jp

Keywords: DEC1, PPAR, RXR, PPRE, obesity, lipid metabolism, thermogenesis, energy homeostasis, circadian rhythms, UCP1

Short title: DEC1 regulates lipid metabolism

ABSTRACT

Obesity is a major public health problem in developed countries resulting from increased food intake and decreased energy consumption and usually associated with abnormal lipid metabolism. Here we show that DEC1, a basic helix-loop-helix transcription factor, plays an important role in the regulation of lipid consumption in mouse brown adipose tissue (BAT), which is the major site of thermogenesis. Homozygous *Dec1* deletion attenuated high-fat-diet-induced obesity, adipocyte hypertrophy, fat volume, and hepatic steatosis. Furthermore, DEC1 deficiency increased body temperature during daytime and enhanced the expression of uncoupler protein 1, a key factor of thermogenesis, and various lipolysis-related genes in interscapular BAT. *In vitro* experiments suggested that DEC1 suppresses the expression of various lipolysis-related genes induced by the heterodimer of peroxisome proliferator-activated receptor γ and retinoid X receptor α (RXRα) through direct binding to RXRα. These observations suggest that enhanced lipolysis in BAT caused by DEC1 deficiency leads to an increase in lipid consumption, thereby decreasing lipid accumulation in adipose tissues and the liver. Thus, DEC1 may serve as an energy-saving factor that suppresses lipid consumption, which may be relevant to managing obesity.

1 INTRODUCTION

Obesity is a major risk factor for many chronic diseases, including cardiovascular disease, lipid disorders, atherosclerosis, hypertension, and diabetes (Klein *et al.* 2004). The cause of obesity is the disruption of the balance between intake and consumption of lipids and carbohydrates. Modulation of lipid metabolism, which is under the control of peroxisome proliferator-activated receptor (PPAR) (Lefterova *et al.* 2008; Nielsen *et al.* 2008), is considered a promising therapeutic target for preventing obesity and/or its related diseases. In addition, the regulation of lipid metabolism is closely related to energy homeostasis in the body.

Energy homeostasis, including nutrient metabolism and thermogenesis, is subject to circadian regulation (Cagampang & Bruce 2012; Mohawk *et al.* 2012; Shostak *et al.* 2013). The molecular clock system regulates the circadian rhythms of the sleep-wake and feeding cycles, affecting energy homeostasis in various tissues including adipose tissues (Mohawk *et al.* 2012; Shostak *et al.* 2013). Several studies have shown that clock components, such as CLOCK and BMAL1, are involved in the regulation of adipogenesis and lipogenesis, and these factors are consequently also related to obesity (Turek *et al.* 2005; Zanquetta *et al.* 2010; Paschos *et al.* 2012). In addition, another clock regulator PER2 controls lipid metabolism by interacting with PPARγ (Grimaldi *et al.* 2010). These facts suggest that the clock system plays a role in the development of obesity through the disruption of lipid homeostasis.

The basic helix-loop-helix transcription factor, DEC1 (also known as BHLHE40, Stra13, or Sharp2), and the structurally related protein, DEC2 (also known as BHLHE41 or Sharp1), are ubiquitously expressed and implicated in neurogenesis (Rossner *et al.* 1997), cell growth arrest (Sun & Taneja 2000), chondrogenesis (Shen *et al.* 2002), and carcinogenesis (Miyazaki *et al.* 2002). DEC1 and DEC2, the expression of which is regulated by the CLOCK:BMAL1 heterodimer through the CACGTG E-box, are also involved in a core feedback loop of the molecular clock system (Honma *et al.* 2002; Nakashima *et al.* 2008; Kato *et al.* 2014). In addition, our previous study showed that forced expression of DEC1 suppressed the adipogenic differentiation of human mesenchymal stem cells (Iwata *et al.* 2006). Other studies have also reported the involvement of DEC1 in adipogenesis (Yun *et al.* 2002; Park & Park 2012). These findings suggest that DEC1 plays an important role in the control of adipogenesis and lipid metabolism.

In this study, we show that DEC1 deficiency prevents obesity in mice fed a high-fat diet. We also demonstrate that DEC1 suppresses the expression of lipolysis-related genes in brown adipose tissue (BAT) through binding to the PPARγ: retinoid X receptor α (RXRα) heterodimer, which is a key regulator of adipogenesis and lipid metabolism (Lefterova *et al.* 2008; Nielsen *et al.* 2008; Wakabayashi *et al.* 2009).

2 RESULTS

2.1 DEC1 deficiency attenuates high-fat-diet-induced obesity.

In our previous study, we established *Dec1*$^{-/-}$ mice (Nakashima *et al.* 2008), and confirmed *Dec1* deficiency in the adipose tissues and liver used in this study (see Figure 3b). Although DEC1 has been suggested to be involved in adipogenic differentiation (Yun *et al.* 2002; Iwata *et al.* 2006; Park & Park 2012), the body weight of *Dec1*$^{-/-}$ mice is almost the same as that of wild-type (WT) mice (Figure 1a). We therefore assessed whether DEC1 deficiency affects obesity or other disorders related to lipid metabolism when mice are fed a high-fat diet. When fed such a diet from 4 weeks of age, *Dec1*$^{-/-}$ mice gained less weight than WT mice, and the difference became more pronounced with age (Figure 1a) even though food intake per body weight by these mice was similar throughout the experimental period (data not shown).

To assess the increase in the volumes of subcutaneous and visceral fat, we investigated the distribution of fat depots in the abdomen of 14-week-old mice (10 weeks into the feeding diet) using micro-computed tomography (micro-CT). The abdominal mid-section between the L1–L6 lumbar vertebrae, which correlates with total adiposity and explanted fat pad weight (Lubura *et al.* 2012), was selected for this analysis; the total and fat volumes of this region were significantly smaller in *Dec1*$^{-/-}$ mice than in WT on both control and high-fat diets (Figure 1b,c). Taken together, these data suggest that DEC1 deficiency suppresses the body weight gain, probably due to the decrease in lipid accumulation, although body weight gain was not significantly different between WT and *Dec1*$^{-/-}$ mice on the control diet.

2.2 DEC1 deficiency reduces lipid accumulation in white adipose tissue (WAT), BAT, and liver.

Histological examination showed that adipocytes in WAT became hypertrophic in both WT and *Dec1*$^{-/-}$ mice fed a high-fat diet (Figure 1d). However, adipocytes in *Dec1*$^{-/-}$ mice were apparently smaller than those in WT. Average sizes of adipocytes in WAT were 68.5 ± 0.6 and 49.9 ± 0.5 μm in WT and *Dec1*$^{-/-}$ mice fed a control diet, respectively; and 103.0 ± 1.1

and 86.9 ± 0.9 in WT and *Dec1*$^{-/-}$ mice fed a high-fat diet, respectively (Figure 1e). Thus, DEC1 deficiency significantly reduced adipocyte size in mice fed both control and high-fat diets compared with the WT mice under the same dietary regimens.

Decreased lipid accumulation was observed in the BAT of *Dec1*$^{-/-}$ mice in both control and high-fat diet groups compared with WT mice (Figure 1f,g). The lipid-accumulated area in the liver was also smaller in *Dec1*$^{-/-}$ mice fed a high-fat diet than that in WT mice (Figure 1h,i). In addition, when fed a high-fat diet, WT mice appeared to develop severe hepatic steatosis compared with *Dec1*$^{-/-}$ mice (Figure 1j). These findings suggest that DEC1 deficiency prevents obesity through decreased lipid accumulation in adipose tissues and the liver.

2.3 DEC1 deficiency increases body temperature and *Ucp1* expression in BAT.

It is likely that increased energy consumption in the body attenuates obesity or hepatic steatosis in *Dec1*$^{-/-}$ mice. Since DEC1 is a member of the molecular clock system (Honma *et al.* 2002; Kato *et al.* 2014), it is necessary to examine the effect of DEC1 deficiency at least twice a day. Consequently, we measured the core temperature of mice at Zeitgeber time (ZT) 2 and ZT14, corresponding to the times of trough and peak core temperatures, respectively, in normal mice (Hannibal *et al.* 2011). The core temperature at ZT14 was almost equal in the four groups of mice, irrespective of diet or genotype. However, the core temperature of *Dec1*$^{-/-}$ mice at ZT2, which is the resting phase during the daytime, was significantly higher than that of WT mice on both diets (Figure 2a).

In *Dec1*$^{-/-}$ mice fed a high-fat diet, the core temperature at ZT2 and ZT14 was almost the same (Figure 2a). The increase in the core temperature of *Dec1*$^{-/-}$ mice over WT at ZT2 suggested that energy consumption and thermogenesis, which are crucial for body temperature control, were enhanced. Therefore, we examined the expression of uncoupling protein 1 (*Ucp1*), which is preferentially expressed in BAT and is responsible for thermogenesis (Richard & Picard 2011). *Ucp1* expression increased in the BAT of WT and *Dec1*$^{-/-}$ mice fed a high-fat diet; *Ucp1* levels were higher in *Dec1*$^{-/-}$ mice than in WT under the same dietary condition (Figure 2b). The increase in *Ucp1* expression in the BAT of *Dec1*$^{-/-}$ mice fed a high-fat diet was more prominent at ZT2, which is the time point at which the core temperature was elevated.

2.4 DEC1 deficiency increases gene expression related to lipid metabolism in BAT.

Since UCP1-dependent thermogenesis requires the supply of lipids as substrates (Cannon & Nedergaard 2004), we examined the expression of the following lipolysis-related genes: lipoprotein lipase (*Lpl)*, a gene involved in the uptake of fatty acid from the plasma into cells (Schoonjans *et al.* 1996); carnitine palmitoyltransferase 1b (*Cpt1b*), an essential gene for the uptake of fatty acids into mitochondria for β-oxidation (Zhang *et al.* 2016); cytochrome c oxidase subunit IV (*Cox4*) and ATP synthase F1 complex β subunit (*Atp5b*), genes coding for mitochondrial electron transport proteins (Sun *et al.* 2015); several isoforms of acyl-CoA dehydrogenase (*Acad1*, *Acad4*, and *Acad6*), genes of key enzymes in fatty acid β-oxidation (Gulick *et al.* 1994); and *Pparγ*, a key transcription factor gene involved in lipid metabolism. In both genotypes, the high-fat diet enhanced the expression of most of these genes in BAT (Figure 3a). DEC1 deficiency also increased their mRNA levels at ZT2 or ZT14, or both. In contrast, transcript levels of these genes in WAT and liver were very low and did not significantly differ between the two genotypes, irrespective of the diet, although *Lpl* and *Pparγ* were also expressed at high levels in WAT.

Thus, DEC1 deficiency significantly increased the expression of *Ucp1* as well as genes involved in fatty acid β-oxidation and mitochondrial energy metabolism in BAT, likely causing the higher body temperature (Figure 2b) and decreased fat depots (Figure 1b,c) observed in these animals. DEC2 (a DEC1 isoform) could not compensate for DEC1-deletion in BAT because *Dec2* expression was not upregulated in the BAT of *Dec1*$^{-/-}$ mice (Figure 3b).

2.5 DEC1 directly suppresses the activity of the PPARγ:RXRα heterodimer.

Next, the underlying mechanism by which DEC1 affects gene expression was investigated. *Ucp1*, *Acad1*, *Acad4*, and *Acad6*, along with *Cpt1b*, *Cox4 Atp5b*, and *Lpl*, which showed altered expression in the BAT of *Dec1*$^{-/-}$ mice (see above), are targets of PPARγ (Lefterova *et al.* 2008; Nielsen *et al.* 2008; Wakabayashi *et al.* 2009). Because PPARγ induces transcription of these genes by binding to PPAR responsive elements (PPREs) as a heterodimer with RXRα, we examined whether DEC1 modulates the transcriptional activity of the consensus PPRE (Lemay & Hwang 2006) in the presence of the PPARγ:RXRα heterodimer using luciferase reporter assays. The luciferase activity of the consensus PPRE reporter was enhanced by the PPARγ:RXRα heterodimer in 3T3-L1 differentiated adipocytes; the transactivation by the PPARγ:RXRα heterodimer was significantly

suppressed by DEC1, although the activity of the reporter was not affected by DEC1 alone (Figure 4a).

To examine the interaction of DEC1 with PPARγ target genes in cells, we performed chromatin immunoprecipitation (ChIP) assays using 3T3-L1 cells; anti-DEC1 antibodies; and primer sets for the *Lpl*, perilipin 1 (*Plin1*: lipid droplet associated protein), and *Pparγ* genes (Schoonjans *et al.* 1996; Nagai *et al.* 2004). Using the anti-DEC1 immunoprecipitates or the input samples from 3T3-L1 adipocytes as a template, PCR products with the expected sizes for the respective PPRE regions were generated (Figure 4b). These findings demonstrate that DEC1 binds to the PPRE region of PPARγ target genes in cells, probably through binding to the PPARγ:RXRα heterodimer.

Cho *et al.* (2009) have already demonstrated that DEC1 suppresses transcriptional activation by nuclear receptors such as liver X receptor α, farnesoid X receptor, vitamin D receptor, and retinoic acid receptor α through direct binding to their heterodimerization partner, RXRα. We therefore examined whether DEC1 binds to PPARγ or RXRα to inhibit the activity of the PPARγ:RXRα heterodimer. We transfected expression plasmids for FLAG-DEC1, RXRα, and PPARγ into human embryonic kidney (HEK) 293 cells and examined their interaction by immunoprecipitation using anti-FLAG antibodies. RXRα coprecipitated with FLAG-DEC1, whereas PPARγ was detected only in the presence of both FLAG-DEC1 and RXRα (Figure 4c), indicating that DEC1 directly associates with RXRα, but not with PPARγ. These results, together with those of the luciferase reporter (Figure 4a) and ChIP (Figure 4b) assays, demonstrate that DEC1 interacts with RXRα at the PPREs in the PPARγ target genes, and thereby suppresses PPARγ:RXRα heterodimer-induced transactivation.

3 DISCUSSION

Here, we examined the effects of DEC1 deficiency on obesity-related phenotypes such as body weight gain, lipid accumulation, and thermogenesis in mice. The body weight of *Dec1*$^{-/-}$ mice fed a high-fat diet was lower than that of WT mice maintained under the same conditions; fat volume in the abdomen of *Dec1*$^{-/-}$ mice was significantly smaller than that of WT. In addition, body temperature increased in *Dec1*$^{-/-}$ mice compared with WT mice. Correspondingly, the expression of various lipid-metabolizing genes in *Dec1*$^{-/-}$ mice was upregulated in BAT, the major site of thermogenesis, but not in WAT and the liver. DEC1

suppressed the transcriptional activity of the PPARγ:RXRα-heterodimer, a key transcription factor in lipid metabolism, by directly binding to RXRα. These results suggest that DEC1 is a potent regulator of lipid and energy metabolism, and that suppressive regulation by DEC1 via binding to the PPARγ:RXRα heterodimer is an effective way to save lipid energy.

Genome-wide analyses identified more than 5,000 binding sites of the PPARγ:RXRα heterodimer in adipocytes (Lefterova *et al.* 2008; Nielsen *et al.* 2008; Wakabayashi *et al.* 2009). Most lipid-metabolizing genes influenced by DEC1 deficiency are included in the lists of PPARγ target genes in those reports. Figure 5 illustrates the possible effects of DEC1 deficiency in reducing the development of obesity by the transcriptional regulation of PPARγ target genes via PPREs involved in lipid consumption in BAT, the lipid flow from WAT to BAT, and the accumulation of lipid in WAT. DEC1 deletion results in the upregulation of *Ucp1* and many lipolysis-related genes responsible for β-oxidation (*Acad*), lipid transport (*Lpl* and *Cpt1b*) and electron transport (*Cox4* and *Atp5b*) in BAT, leading to increased lipid consumption and thermogenesis, which require the enhancement of lipid supply from WAT to BAT. A recent study has demonstrated that BAT is a master regulator of triglyceride clearance: it efficiently consumes fatty acids according to a metabolic program (Bartelt *et al.* 2011). Accelerated lipid intake and consumption in the BAT of *Dec1*$^{-/-}$ mice may result in a decrease in lipid accumulation and adipocyte size in WAT, leading to the prevention of obesity. In addition, the increased consumption of lipids in DEC1-deficient BAT appears to reduce the development of hepatic steatosis, the ectopic accumulation of lipids in the liver.

Similar to this study, Cho *et al*. (2009) demonstrated that DEC1 could bind to RXRα via an LxxLL motif in DEC1, a motif typically found in cofactors of nuclear receptors (Rosenfeld *et al.* 2006), to repress the transactivation activity of nuclear receptors that function with RXRα as a partner, such as the liver X receptor α, farnesoid X receptor, vitamin D receptor, and retinoic acid receptor α, although *in vivo* effects were not demonstrated. The results in this study demonstrate that DEC1 represses the transactivation activity of another partner of RXRα, i.e., PPARγ, and thereby regulates lipid metabolism in BAT. To our knowledge, this is the first report to illustrate the *in vivo* action of DEC1 through binding to RXRα.

Most lipid-metabolizing genes examined in the present study were expressed at high levels and influenced by DEC1 deficiency in BAT, whereas the same genes were expressed at low levels and not necessarily affected by DEC1 deficiency in the liver. These differences may be partly due to the minor contribution of PPARγ to the regulation of lipid metabolism

in the liver. In fact, the expression of *Pparγ* was substantially lower in the liver than in BAT. In addition, DEC2 may compensate for the loss of DEC1, because *Dec2* expression was markedly upregulated in the *Dec1*$^{-/-}$ liver. These findings may explain why we observed no significant differences in the transcript levels of hepatic genes for lipid metabolism upon DEC1 deficiency. Although most hepatic genes examined in the present study are PPARγ target genes, there may be additional regulatory factors controlling these genes, which need to be elucidated in future studies.

Various physiological functions, including body temperature, exhibit circadian rhythms that are, directly or indirectly, under the control of the master circadian factor, the CLOCK:BMAL1 heterodimer (Mohawk *et al.* 2012). CLOCK:BMAL1 activates clock genes through binding to E-boxes, while DEC1 participates in the circadian regulation by competing with CLOCK:BMAL1 for binding to the same E-boxes (Honma *et al.* 2002; Kawamoto *et al.* 2004). Ohishi *et al.* (2006) reported that the disruption of CLOCK function attenuated high-fat-diet-induced obesity. On the other hand, DEC1 deficiency led to similar results in this study to those reported. In addition, we found that body temperature increased in *Dec1*$^{-/-}$ mice at ZT2, but not at ZT14, when compared with WT mice, resulting in the disruption of the day-night difference. Moreover, all of the PPARγ target genes examined in this study were upregulated in *Dec1*$^{-/-}$ BAT, at least at ZT14. Although the expression of *Dec1*, as well as *Dec2*, exhibited a day-night difference, the expression of most genes governed by PPARγ did not (shown in Figure 3), suggesting that these genes are not direct targets of CLOCK:BMAL1. Therefore, DEC1 may influence circadian rhythms in lipid metabolism-related activities such as thermogenesis through interaction with PPARγ:RXRα, but not through the interaction with CLOCK:BMAL1, suggesting another mechanism underlying the circadian regulation of PPARγ-target genes. In fact, DEC1 deficiency almost disrupted the circadian rhythm of core temperature and prevented high-fat-diet-induced obesity, possibly due to the upregulation of *Ucp1* in ZT2. Further studies are needed to uncover the finer details of the physiological role of DEC1 in lipid metabolism and thermogenesis.

In the present study, we obtained some inconsistent results, reason for which is difficult to explain. First, core temperature in *Dec1*$^{-/-}$ mice was significantly increased in ZT2 but not in ZT14 compared with the WT mice although *Ucp1* expression was upregulated in both ZT2 and ZT14. The time lag between circadian phases of rhythms of *Ucp1* expression and core temperature may explain the observed difference. Several factors other than UCP1 involved

in thermogenesis may also explain this discrepancy. Second, the fat volume of the abdominal region was significantly smaller in *Dec1*$^{-/-}$ mice than in WT mice fed a control or high-fat diet. However, we found no difference in body weight between WT and *Dec1*$^{-/-}$ mice fed a control diet from 5 to 16 weeks although there was a significant decrease in body weight of *Dec1*$^{-/-}$ mice at 4 weeks. Apparently, there are unknown mechanisms compensating these differences through uncharacterized pathways. The increased core temperature and the decreased body weight and fat volume observed in *Dec1*$^{-/-}$ mice could be influenced by increased locomotor activity. However, the observed locomotor activities were not significantly different between WT and *Dec1*$^{-/-}$ mice fed a control diet (unpublished data) although the activities of mice fed a high-fat diet were not examined. Future research should focus on phenotypes other than lipid metabolism under both high-fat and control diet conditions.

In nature, animals often face starvation; obese animals in the natural environment are uncommon. In this context, DEC1 appears to serve as a "energy-saving" factor to survive starvation. However, in the modern human lifestyle, energy-saving factors such as DEC1 may promote obesity under excess nutrition conditions. In addition, DEC1 can be induced by environmental stimuli such as light and feeding (Honma *et al.* 2002; Kawamoto *et al.* 2006; Kato *et al.* 2014), and this elevated DEC1 expression may further promote obesity. We anticipate that our findings may provide new therapeutic and prophylactic avenues for the prevention and mitigation of obesity-related diseases.

4 EXPERIMENTAL PROCEDUERS

4.1 Animals.

Male C57BL/6J WT and *Dec1*$^{-/-}$ mice (Nakashima *et al.* 2008) were housed under a 12-h light/dark cycle at a constant temperature and given food and water *ad libitum*. All manipulations during the dark phase were performed using night vision goggles (Bushnell Corp.) or under a red dim light to avoid disruptions of circadian rhythms. All procedures were performed in compliance with standard principles and guidelines for the care and use of laboratory animals at Hiroshima University Institute of Biomedical and Health Sciences under the ethical permission of Animal Research Committee of Hiroshima University.

For the high-fat diet experiment, 4-week-old male WT and *Dec1*$^{-/-}$ mice were divided into two groups that were fed either a high-fat diet (82% kcal fat, 15% kcal protein, and 3% kcal carbohydrate; F2HFHSD; Oriental Yeast Co. Ltd) or a control diet (40.6% kcal fat,

17.6% kcal protein, and 41.8% kcal carbohydrate; AIN93G). Mice were differentiated by ear punches. Weight and core temperature were measured weekly and core temperature was monitored using a BAT-12 Microprobe Thermometer equipped with a rectal probe for mice (Muromachi Kikai Co., Ltd). After 10–13 weeks, mice were scanned by micro-CT or sacrificed and subjected to histological analysis and RNA extraction.

4.2 Isolation of RNA and quantitative real-time RT-PCR analysis.

At 13 weeks after the initiation of the feeding experiment, 4-5 mice from each group were decapitated at the indicated time points in a normal light/dark cycle. All RNA preparations were obtained separately from visceral WAT, interscapular BAT, and liver of individual mice, and used to measure the transcript levels of various genes, as described previously (Ozaki *et al.* 2012).

Quantitative real-time RT-PCR analysis was performed using the ABI PRISM 7900 Sequence Detection System (Applied Biosystems) as described (Gibson *et al.* 1996). First strand cDNA synthesis, and the sequences of the primers and TaqMan™ fluorogenic probes (Applied Biosystems) for mouse *Dec1* and *Dec2* have been described previously (Noshiro *et al.* 2005). The sequences of the primers and TaqMan™ fluorogenic probes for the other genes were designed using the ProbeFinder™ software of the Roche Universal Probe Library system (Roche Applied Science). The sequences and probe IDs are listed in Table 1.

4.3 Micro-CT scan analysis of mouse fat.

At 10 weeks after the initiation of the feeding experiment, mice were anesthetized by an intraperitoneal injection of pentobarbital (50 mg/kg body weight) and positioned with both legs fully extended. The body of each mouse was scanned at 36 μm with a SkyScan 1176-HT (SkyScan Co.). 2D image slices of the abdominal region (between the proximal end of the first lumbar vertebra and the distal end of the sixth lumbar vertebra) were reconstructed into a 3D tomography image as shown in Figure 1b. The reconstituted visceral and subcutaneous fat depots were visualized and quantified by CT-Vol and CT-An software (SkyScan Co.).

4.4 Histological analysis.

Formalin-fixed visceral WAT, interscapular BAT, and liver were imbedded in paraffin, and 4-μm thick sections were stained with hematoxylin and eosin using 17-week-old mice. Sections were analyzed at ×100 magnification using an Eclipse 80i microscope (Nikon Corp.),

and digital images (1,280 × 960 pixels) were obtained using NIS Elements D image analysis software (Nikon Corp.). The adipocytes' sizes were determined with Lumina Vision 2.20 (Mitani Inc.), measuring at least 1000 cells from each group of 8–10 mice. Oil droplet areas in BAT and liver were also measured with the same software.

4.5 Luciferase reporter assay.

Double-stranded DNA fragments containing three repeats of the PPRE consensus sequence (AGGTCAAAGGTCA) (Ijpenberg *et al.* 1997) were prepared by annealing the oligonucleotide pair of the consensus PPRE shown below. The fragments were used to construct a reporter plasmid using pGL4 with a minimal promoter (Promega). The construction of the expression plasmid (pcDNA3.1) for mouse DEC1 has been described previously (Noshiro *et al.* 2004). The expression plasmids (pCMX) for mouse PPARγ and human RXRα were kindly supplied by Dr. M. Makishima (Nihon University, Japan). The oligonucleotides used for the consensus PPRE × 3 were upper strand: 5′-CTAGCAGGGGACCAGGACAAAGGTCACGTTCGGGAGTCGACAGGGGACCAGGA CAAAGGTCACGTTCGGGAGTCGACAGGGGACCAGGACAAAGGTCACGTTCGGGA -3′, and lower strand: 5′-TCGATCCCGAACGTGACCTTTGTCCTGGTCCCCTGCGACTCCCGAACGTGACCTTT GTCCTGGTCCCCTGTCGACTCCCGAACGTGACCTTTGTCCTGGTCCCCTG-3′.

Mouse 3T3-L1 cells were inoculated at 1×10^4 cells/well in 96-well plastic plates and cultured in Dulbecco's modified Eagle's medium (Sigma-Aldrich) containing 1 mg/ml D-glucose, 10% (v/v) fetal bovine serum (FBS) (HyClone), 50 μg/ml ascorbic acid, 32 U/ml penicillin and 40 μg/ml streptomycin at 37°C in a 5% CO_2 incubator. For adipogenic differentiation of 3T3-L1 preadipocytes, the medium was changed to adipogenic induction medium containing 5% FBS, 1 μM dexamethasone (Sigma-Aldrich), 500 μM 3-isobutyl-1-methylxanthine (Wako), 200 μM indomethacin (Wako), 5 μM troglitazone (Wako), and 10 μg/ml insulin (Wako) (Pittenger *et al.* 1999). The medium was replaced with adipogenesis maintenance medium containing 10% FBS and 10 μg/ml insulin every 2 days after adipogenic induction. 3T3-L1 adipocytes were used for reporter assays 6 days after induction. DNA transfection of the luciferase constructs with the internal control plasmid pRL-TK and the expression plasmids was performed using Lipofectamine-LTX transfection reagent (Life Technologies). The ligands troglitazone (1 μM) and 9-cis retinoic acid (0.1 μM) for PPARγ and RXRα, respectively, dissolved in dimethyl sulfoxide, were added to the culture medium

(Gottlicher *et al.* 1992; Willy *et al.* 1995). Two days after transfection, the cells were harvested and the cell lysate was analyzed using dual luciferase assay reagents (Promega). Three wells were measured for each assay, and luciferase activities were normalized against internal control values. Two independent transfection experiments were performed.

4.6 ChIP assay.

ChIP assays of PPRE using anti-DEC1 antibodies (Nakashima *et al.* 2008) were performed using a ChIP Assay Kit (Upstate) according to the manufacturer's instructions. Differentiating 3T3-L1 adipocytes were used 6 days after induction. Cellular genomic DNA was cross-linked with formaldehyde and sonicated. DNA fragments were precipitated using anti-DEC1 antibodies (αDEC1) or control IgG (Co IgG). DNA samples recovered from 3T3-L1 adipocytes were subjected to PCR using the gene specific primers listed below, to detect DEC1 binding to the PPRE region of *Pparγ*, *Lpl*, and *Plin1* (Schoonjans *et al.* 1996; Nagai *et al.* 2004). The PCR primers used were as follows: *Pparγ*, 5′-GTTAGCAGTTTGGCACAGCTAGGT-3′ and 5′-AAAATTGGAGCCCTCCCTGAGA-3′; *Lpl*, 5′-CGGTAGGCAAACTGGAGTCTAAAC-3′ and 5′-GCAGAACAGTTACAAGGGGCAGAA-3′; *Plin1*, 5′-ATCATAGTCCCCGGCTGTTAAGCA-3′ and 5′-TGGGTGAAAGGTGACAAGGGAAAG-3′.

4.7 Immunoprecipitation assay.

HEK293 cells were cultured in Dulbecco's modified Eagle's medium containing 5% FBS, 100 U/ml penicillin, and 100 μg/ml streptomycin at 37°C in a humidified atmosphere containing 5% CO_2. HEK293 cells in a 10-cm dish were transfected with various combinations of pFLAG-DEC1, pFLAG-CMV2, pCMX-RXRα, and pCMX-PPARγ using Lipofectamine 2000 (Invitrogen). Twenty-four hours after transfection, cells were harvested with lysis buffer (20 mM Tris-HCl, pH 8.0, 150 mM NaCl, 5 mM EDTA, 1% NP-40) containing complete protease inhibitor cocktail (Roche). The lysates were mixed with anti-FLAG Sepharose 4B beads (Sigma-Aldrich) in the presence of a ligand (5 μM troglitazone) and rotated for 2 h at 4°C. The beads were washed three times with cold lysis buffer. The bound proteins were eluted by boiling in SDS sample buffer and were analyzed by immunoblotting with anti-DEC1 (Nakashima *et al.* 2008), anti-PPARγ (Cell Signaling Technologies, #2443) or anti-RXRα antibodies (Cell Signaling Technologies, #5388). The

immunoreactive proteins were visualized using IRDye® Secondary Antibody and the Odyssey® Infrared Imaging System (Li-Cor Biosciences).

4.8 Statistical analysis.

Results were expressed as mean ± SEM. We assessed the results by the Student's t-test for comparing two groups, or by two-way ANOVA for multiple comparisons. A P value less than 0.05 was considered significant.

ACKNOWLEDGMENTS

We are grateful to Dr. Makoto Makishima for helpful discussions. We thank Drs. Urara Fukuzaki-Dohi, Kazuko Kitayama, Noriko Goto, Ronald Veronica Sainik, and Misa Takeyasu for their technical support. This work was supported by Grants-in-Aid for Science from the Japan Society for the Promotion of Science (grant numbers 22590223 and 2339042351). The authors declare that they have no conflicts of interest.

REFERENCES

Bartelt, A., Bruns, O.T., Reimer, R., Hohenberg, H., Ittrich, H., Peldschus, K., ... Heeren, J. (2011) Brown adipose tissue activity controls triglyceride clearance. *Nature Medicine 17*, 200-205. 10.1038/nm.2297

Cagampang, F.R. & Bruce, K.D. (2012) The role of the circadian clock system in nutrition and metabolism. *British Journal of Nutrition 108*, 381-392. 10.1017/S0007114512002139

Cannon, B. & Nedergaard, J. (2004) Brown adipose tissue: function and physiological significance. *Physiological Reviews 84*, 277-359. 10.1152/physrev.00015.2003

Cho, Y., Noshiro, M., Choi, M., Morita, K., Kawamoto, T., Fujimoto, K., ... Makishima, M. (2009) The basic helix-loop-helix proteins differentiated embryo chondrocyte (DEC) 1 and DEC2 function as corepressors of retinoid X receptors. *Molecular Pharmacology 76*, 1360-1369. 10.1124/mol.109.057000

Gibson, U.E., Heid, C.A. & Williams, P.M. (1996) A novel method for real time quantitative RT-PCR. *Genome Research 6*, 995-1001.

Gottlicher, M., Widmark, E., Li, Q. & Gustafsson, J.A. (1992) Fatty acids activate a chimera of the clofibric acid-activated receptor and the glucocorticoid receptor. *Proceedings of the National Academy of Sciences, U S A 89*, 4653-4657.

Grimaldi, B., Bellet, M.M., Katada, S., Astarita, G., Hirayama, J., Amin, R.H., ... Sassone-Corsi, P. (2010) PER2 controls lipid metabolism by direct regulation of PPARgamma. *Cell Metabolism 12*, 509-520. 10.1016/j.cmet.2010.10.005

Gulick, T., Cresci, S., Caira, T., Moore, D.D. & Kelly, D.P. (1994) The peroxisome proliferator-activated receptor regulates mitochondrial fatty acid oxidative enzyme gene expression. *Proceedings of the National Academy of Sciences, U S A 91*, 11012-11016.

Hannibal, J., Hsiung, H.M. & Fahrenkrug, J. (2011) Temporal phasing of locomotor activity, heart rate rhythmicity, and core body temperature is disrupted in VIP receptor 2-deficient mice. *American Journal of Physiology: Regulatory, Integrative and Comparative Physiology 300*, R519-530. 10.1152/ajpregu.00599.2010

Honma, S., Kawamoto, T., Takagi, Y., Fujimoto, K., Sato, F., Noshiro, M., ... Honma, K. (2002) Dec1 and Dec2 are regulators of the mammalian molecular clock. *Nature 419*, 841-844. 10.1038/nature01123

Ijpenberg, A., Jeannin, E., Wahli, W. & Desvergne, B. (1997) Polarity and specific sequence requirements of peroxisome proliferator-activated receptor (PPAR)/retinoid X receptor heterodimer binding to DNA. A functional analysis of the malic enzyme gene PPAR response element. *The Journal of Biological Chemistry 272*, 20108-20117.

Iwata, T., Kawamoto, T., Sasabe, E., Miyazaki, K., Fujimoto, K., Noshiro, M., ... Kato, Y. (2006) Effects of overexpression of basic helix-loop-helix transcription factor Dec1 on osteogenic and adipogenic differentiation of mesenchymal stem cells. *European Journal of Cell Biology 85*, 423-431. 10.1016/j.ejcb.2005.12.007

Kato, Y., Kawamoto, T., Fujimoto, K. & Noshiro, M. (2014) DEC1/STRA13/SHARP2 and DEC2/SHARP1 Coordinate Physiological Processes, Including Circadian Rhythms in Response to Environmental Stimuli. *Current Topics in Developmental Biology 110*, 339-372. 10.1016/B978-0-12-405943-6.00010-5

Kawamoto, T., Noshiro, M., Furukawa, M., Honda, K.K., Nakashima, A., Ueshima, T., ... Kato, Y. (2006) Effects of fasting and re-feeding on the expression of Dec1, Per1, and other clock-related genes. *Journal of Biochemistry (Tokyo) 140*, 401-408. 10.1093/jb/mvj165

Kawamoto, T., Noshiro, M., Sato, F., Maemura, K., Takeda, N., Nagai, R., ... Kato, Y. (2004) A novel autofeedback loop of Dec1 transcription involved in circadian rhythm regulation. *Biochemical and Biophysical Research Communications 313*, 117-124. 10.1016/j.bbrc.2003.11.099

Klein, S., Sheard, N.F., Pi-Sunyer, X., Daly, A., Wylie-Rosett, J., Kulkarni, K. & Clark, N.G. (2004) Weight management through lifestyle modification for the prevention and management of type 2 diabetes: rationale and strategies. A statement of the American Diabetes Association, the North American Association for the Study of Obesity, and the American Society for Clinical Nutrition. *American Journal of Clinical Nutrition 80*, 257-263.

Lefterova, M.I., Zhang, Y., Steger, D.J., Schupp, M., Schug, J., Cristancho, A., ... Lazar, M.A. (2008) PPARgamma and C/EBP factors orchestrate adipocyte biology via adjacent binding on a genome-wide scale. *Genes & Development 22*, 2941-2952. 10.1101/gad.1709008

Lemay, D.G. & Hwang, D.H. (2006) Genome-wide identification of peroxisome proliferator response elements using integrated computational genomics. *Journal of Lipid Research 47*, 1583-1587. 10.1194/jlr.M500504-JLR200

Lubura, M., Hesse, D., Neumann, N., Scherneck, S., Wiedmer, P. & Schurmann, A. (2012) Non-invasive quantification of white and brown adipose tissues and liver fat content by computed tomography in mice. *PLoS One 7*, e37026. 10.1371/journal.pone.0037026

Miyazaki, K., Kawamoto, T., Tanimoto, K., Nishiyama, M., Honda, H. & Kato, Y. (2002) Identification of functional hypoxia response elements in the promoter region of the DEC1 and DEC2 genes. *The Journal of Biological Chemistry 277*, 47014-47021. 10.1074/jbc.M204938200

Mohawk, J.A., Green, C.B. & Takahashi, J.S. (2012) Central and peripheral circadian clocks in mammals. *Annual Review of Neuroscience 35*, 445-462. 10.1146/annurev-neuro-060909-153128

Nagai, S., Shimizu, C., Umetsu, M., Taniguchi, S., Endo, M., Miyoshi, H., ... Koike, T. (2004) Identification of a functional peroxisome proliferator-activated receptor responsive element within the murine perilipin gene. *Endocrinology 145*, 2346-2356. 10.1210/en.2003-1180

Nakashima, A., Kawamoto, T., Honda, K.K., Ueshima, T., Noshiro, M., Iwata, T., ... Kato, Y. (2008) DEC1 modulates the circadian phase of clock gene expression. *Molecular and Cellular Biology 28*, 4080-4092. 10.1128/MCB.02168-07

Nielsen, R., Pedersen, T.A., Hagenbeek, D., Moulos, P., Siersbaek, R., Megens, E., ... Stunnenberg, H.G. (2008) Genome-wide profiling of PPARgamma:RXR and RNA polymerase II occupancy reveals temporal activation of distinct metabolic pathways

and changes in RXR dimer composition during adipogenesis. *Genes & Development 22*, 2953-2967. 10.1101/gad.501108

Noshiro, M., Furukawa, M., Honma, S., Kawamoto, T., Hamada, T., Honma, K. & Kato, Y. (2005) Tissue-specific disruption of rhythmic expression of Dec1 and Dec2 in clock mutant mice. *Journal of Biological Rhythms 20*, 404-418. 10.1177/0748730405280195

Noshiro, M., Kawamoto, T., Furukawa, M., Fujimoto, K., Yoshida, Y., Sasabe, E., ... Kato, Y. (2004) Rhythmic expression of DEC1 and DEC2 in peripheral tissues: DEC2 is a potent suppressor for hepatic cytochrome P450s opposing DBP. *Genes to Cells 9*, 317-329. 10.1111/j.1356-9597.2004.00722.x

Oishi, K., Atsumi, G., Sugiyama, S., Kodomari, I., Kasamatsu, M., Machida, K. & Ishida, N. (2006) Disrupted fat absorption attenuates obesity induced by a high-fat diet in Clock mutant mice. *FEBS Letters 580*, 127-130. 10.1016/j.febslet.2005.11.063

Ozaki, N., Noshiro, M., Kawamoto, T., Nakashima, A., Honda, K., Fukuzaki-Dohi, U., ... Kato, Y. (2012) Regulation of basic helix-loop-helix transcription factors Dec1 and Dec2 by RORalpha and their roles in adipogenesis. *Genes to Cells 17*, 109-121. 10.1111/j.1365-2443.2011.01574.x

Park, Y.K. & Park, H. (2012) Differentiated embryo chondrocyte 1 (DEC1) represses PPARgamma2 gene through interacting with CCAAT/enhancer binding protein beta (C/EBPbeta). *Molecules and Cells 33*, 575-581. 10.1007/s10059-012-0002-9

Paschos, G.K., Ibrahim, S., Song, W.L., Kunieda, T., Grant, G., Reyes, T.M., ... Fitzgerald, G.A. (2012) Obesity in mice with adipocyte-specific deletion of clock component Arntl. *Nature Medicine 18*, 1768-1777. 10.1038/nm.2979

Pittenger, M.F., Mackay, A.M., Beck, S.C., Jaiswal, R.K., Douglas, R., Mosca, J.D., ... Marshak, D.R. (1999) Multilineage potential of adult human mesenchymal stem cells. *Science 284*, 143-147.

Richard, D. & Picard, F. (2011) Brown fat biology and thermogenesis. *Frontiers in Bioscience 16*, 1233-1260.

Rosenfeld, M.G., Lunyak, V.V. & Glass, C.K. (2006) Sensors and signals: a coactivator/corepressor/epigenetic code for integrating signal-dependent programs of transcriptional response. *Genes & Development 20*, 1405-1428. 10.1101/gad.1424806

Rossner, M.J., Dorr, J., Gass, P., Schwab, M.H. & Nave, K.A. (1997) SHARPs: mammalian enhancer-of-split- and hairy-related proteins coupled to neuronal stimulation. *Molecular and Cellular Neuroscience 9*, 460-475. 10.1006/mcne.1997.0640

Schoonjans, K., Peinado-Onsurbe, J., Lefebvre, A.M., Heyman, R.A., Briggs, M., Deeb, S., ... Auwerx, J. (1996) PPARalpha and PPARgamma activators direct a distinct tissue-specific transcriptional response via a PPRE in the lipoprotein lipase gene. *The EMBO Journal 15*, 5336-5348.

Shen, M., Yoshida, E., Yan, W., Kawamoto, T., Suardita, K., Koyano, Y., ... Kato, Y. (2002) Basic helix-loop-helix protein DEC1 promotes chondrocyte differentiation at the early and terminal stages. *The Journal of Biological Chemistry 277*, 50112-50120. 10.1074/jbc.M206771200

Shostak, A., Husse, J. & Oster, H. (2013) Circadian regulation of adipose function. *Adipocyte 2*, 201-206. 10.4161/adip.26007

Sun, H. & Taneja, R. (2000) Stra13 expression is associated with growth arrest and represses transcription through histone deacetylase (HDAC)-dependent and HDAC-independent mechanisms. *Proceedings of the National Academy of Sciences, U S A 97*, 4058-4063. 10.1073/pnas.070526297

Sun, Y., Qi, Z., He, Q., Cui, D., Qian, S., Ji, L. & Ding, S. (2015) The effect of treadmill training and N-acetyl-l-cysteine intervention on biogenesis of cytochrome c oxidase (COX). *Free Radical Biology and Medicine 87*, 326-335. 10.1016/j.freeradbiomed.2015.06.035

Turek, F.W., Joshu, C., Kohsaka, A., Lin, E., Ivanova, G., McDearmon, E., ... Bass, J. (2005) Obesity and metabolic syndrome in circadian Clock mutant mice. *Science 308*, 1043-1045. 10.1126/science.1108750

Wakabayashi, K., Okamura, M., Tsutsumi, S., Nishikawa, N.S., Tanaka, T., Sakakibara, I., ... Sakai, J. (2009) The peroxisome proliferator-activated receptor gamma/retinoid X receptor alpha heterodimer targets the histone modification enzyme PR-Set7/Setd8 gene and regulates adipogenesis through a positive feedback loop. *Molecular and Cellular Biology 29*, 3544-3555. 10.1128/MCB.01856-08

Willy, P.J., Umesono, K., Ong, E.S., Evans, R.M., Heyman, R.A. & Mangelsdorf, D.J. (1995) LXR, a nuclear receptor that defines a distinct retinoid response pathway. *Genes & Development 9*, 1033-1045.

Yun, Z., Maecker, H.L., Johnson, R.S. & Giaccia, A.J. (2002) Inhibition of PPAR gamma 2 gene expression by the HIF-1-regulated gene DEC1/Stra13: a mechanism for regulation of adipogenesis by hypoxia. *Developmental Cell 2*, 331-341.

Zanquetta, M.M., Correa-Giannella, M.L., Monteiro, M.B. & Villares, S.M. (2010) Body weight, metabolism and clock genes. *Diabetology & Metabolic Syndrome 2*, 53. 10.1186/1758-5996-2-53

Zhang, Y., Fang, X., Dai, M., Cao, Q., Tan, T., He, W., ... Bao, M. (2016) Cardiac-specific down-regulation of carnitine palmitoyltransferase-1b (CPT-1b) prevents cardiac remodeling in obese mice. *Obesity 24*, 2533-2543. 10.1002/oby.21665

FIGURE LEGENDS

FIGURE 1 DEC1 deficiency attenuates obesity and fat mass. (a) Effects of DEC1 deficiency on body weight. Four-week-old WT mice and *Dec1*$^{-/-}$ mice were fed a control (Co) or high-fat (HF) diet for the experimental period. The inserts show the results of the statistical analysis using the values of 16-week-old mice (n = 8–10; ***p* < 0.01; ns, not significant by Student's *t*-test). (b) Representative images from micro-CT scanning of entire mouse bodies (upper image) and reconstituted 3D structures of fat depots (lower image) in the abdominal region of mice. The cross sections at lumbar (L) 5 are shown in the lower images to discriminate adipose tissue. (c) The total abdominal and fat volumes from L1 to L6 were quantified. Values are mean ± SEM (n = 4–6; **p* < 0.05; ***p* < 0.01 by Student's *t*-test). (d, f, h) Microscope images of hematoxylin and eosin-stained sections of visceral white adipose tissue (WAT) (d), interscapular brown adipose tissue (BAT) (f), and liver (h). Scale bars indicate 100 μm (WAT and liver images) and 50 μm (BAT images). (e) Histograms of cell lengths of adipocytes determined for visceral WAT (d). Values are % of total cell numbers calculated from WAT samples of 8-10 mice (***p* < 0.01 by two-way ANOVA). (g, i) Oil droplet areas in BAT (g) and liver (i) were measured, respectively. Values are mean ± SEM (n = 8–10; **p* < 0.05; ***p* < 0.01 by Student's *t*-test). (j) Representative morphology of livers of HF diet mice. Statistical comparison of data between the two genotypes are shown in the figure by red symbols.

FIGURE 2 Thermogenesis is accelerated in *Dec1*$^{-/-}$ mice. (a) Core temperature of 14-week-old mice was measured at ZT2 and ZT14 during the feeding experiment. Values are mean ± SEM (n = 8–10; ***p* < 0.01 by Student's *t*-test). (b) Transcript levels of *Ucp1* in interscapular BAT were determined by real-time RT-PCR at ZT2 and ZT14. Data are shown as mean ± SEM (n = 4–5; **p* < 0.05; ***p* < 0.01 by Student's *t*-test). Statistical comparisons of data between the two genotypes are depicted by red symbols.

FIGURE 3 (a) Expression profiles of various lipolysis-related genes were analyzed by real-time RT-PCR in BAT, WAT, and liver of WT and *Dec1*$^{-/-}$ mice at ZT2 and ZT14. Values are mean ± SEM (n = 4–5; **p* < 0.05; ***p* < 0.01 by Student's *t*-test). (b) Expression profiles of *Dec1 and Dec2* transcripts in BAT, WAT, and liver of WT and *Dec1*$^{-/-}$ mice at ZT2 and

ZT14. Data are expressed as mean ± SEM (n = 4–5; *$p < 0.05$; **$p < 0.01$ by Student's *t*-test). Statistical comparisons of data between the two genotypes are depicted by red symbols.

FIGURE 4 DEC1 interacts with the PPARγ:RXRα heterodimer at the PPAR response element (PPRE). (a) The pGL4 luciferase reporter plasmid (4 ng) carrying three repeats of the consensus PPRE sequence (AGGTCAAAGGTCA) was co-transfected along with the indicated expression plasmids (40 ng of PPARγ and RXRα; 20, 40, or 60 ng of DEC1) into 3T3-L1 adipocytes. The relative luciferase activities are expressed as mean ± SEM (n = 4; *$p < 0.05$; **$p < 0.01$; ns, not significant by Student's *t*-test). Co, control vector only. (b) ChIP assay of PPARγ target genes (*Lpl*, *Plin1*, and *Pparγ*). The input and the immunoprecipitated DNA fragments recovered from 3T3-L1 adipocytes were amplified using primer sets for *Lpl*, *Plin1*, and *Pparγ.* (c) Interaction of DEC1 with RXRα in cells. HEK293 cells were transfected with various combinations of pFLAG-DEC1, pFLAG-CMV2, pCMX-PPARγ, and pCMX-RXRα. The protein complexes in HEK293 cell lysates were pulled down with anti-FLAG antibody-coupled Sepharose beads and analyzed by Western blotting (WB) with anti-DEC1 (αDEC1), anti-RXRα (αRXRα), and anti-PPARγ (αPPARγ) antibodies.

FIGURE 5 Model explaining the effect of DEC1 deficiency. DEC1 regulates lipolysis-related genes in BAT through PPRE by binding to the PPARγ:RXRα heterodimer. The consumption of lipid for energy generation or thermogenesis occurs mostly in BAT, where lipolytic genes are regulated by PPARγ. DEC1 deficiency could activate lipolytic processing (β-oxidation of fatty acids, lipid transport, and electron transport) and thermogenesis by UCP1 in BAT, thereby decreasing lipid accumulation in WAT.

Figure 1

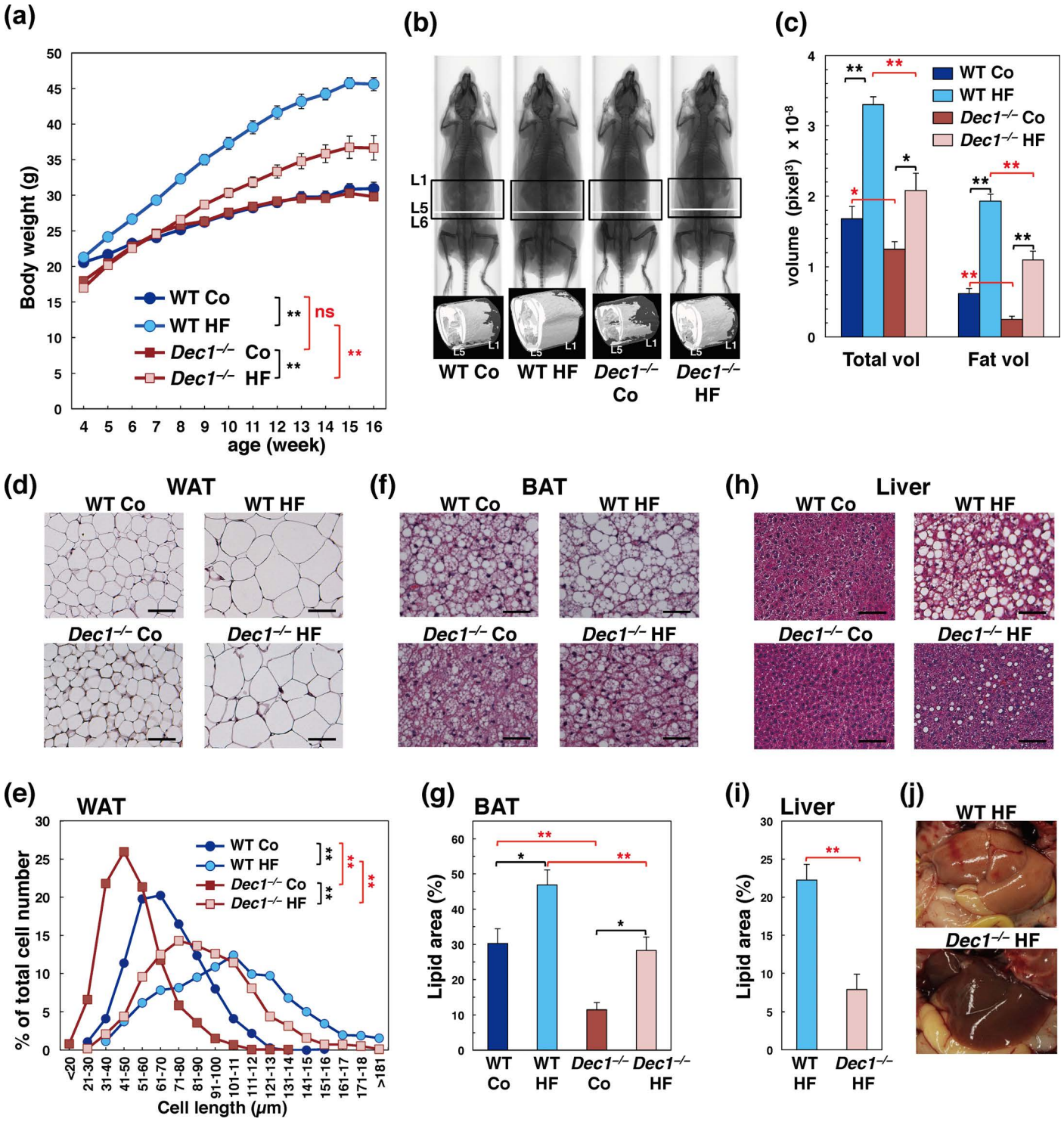
(a)
Body weight (g)
age (week)
WT Co
WT HF
Dec1−/− Co
Dec1−/− HF
ns
(b)
L1
L5
L6
WT Co
WT HF
Dec1−/− Co
Dec1−/− HF
(c)
volume (pixel3) x 10-8
Total vol
Fat vol
(d)
WAT
(e)
WAT
% of total cell number
Cell length (μm)
(f)
BAT
(g)
BAT
Lipid area (%)
(h)
Liver
(i)
Liver
Lipid area (%)
(j)

Figure 2

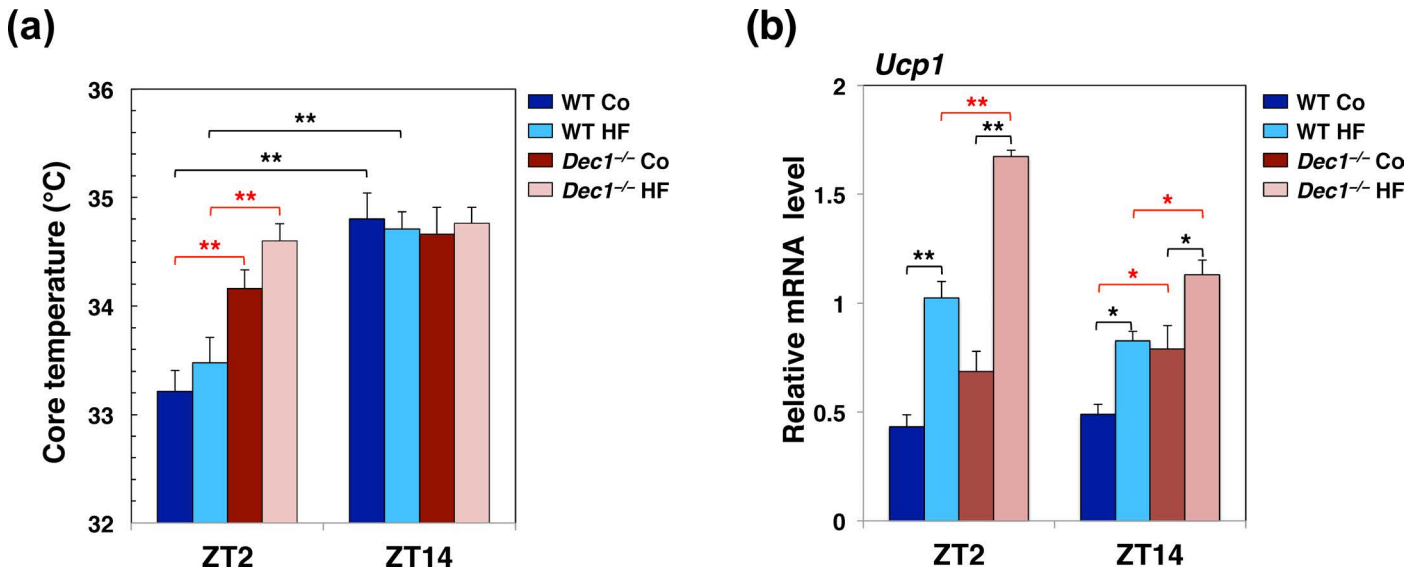
(a)
Core temperature (°C)
36
35
34
33
32
ZT2
ZT14
WT Co
WT HF
Dec1−/− Co
Dec1−/− HF
**
**
**
**
(b)
Ucp1
Relative mRNA level
2
1.5
1
0.5
0
ZT2
ZT14
WT Co
WT HF
Dec1−/− Co
Dec1−/− HF
**
**
**
*
*
*

Figure 3

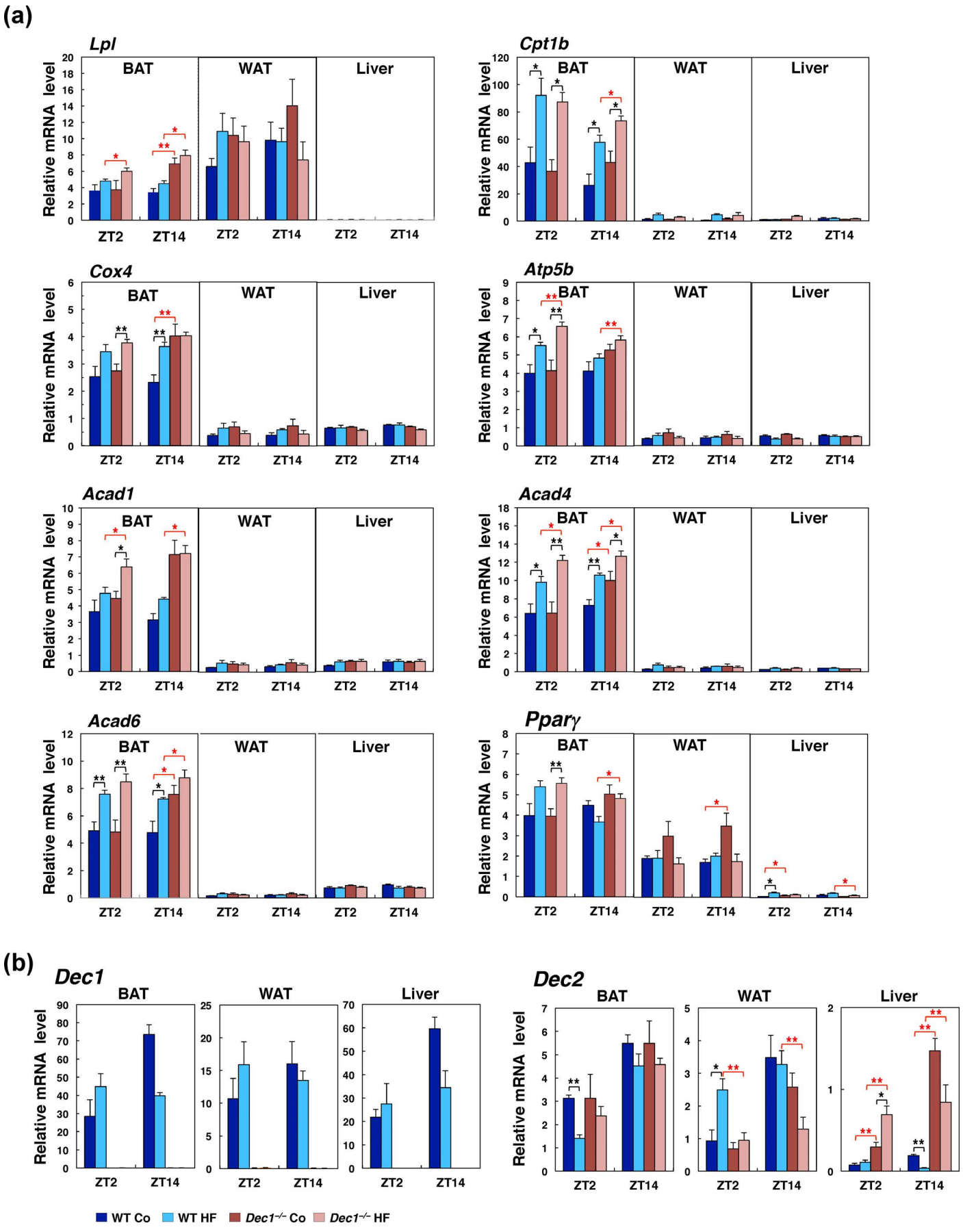
(a)
Lpl
Cpt1b
Cox4
Atp5b
Acad1
Acad4
Acad6
Pparγ
BAT
WAT
Liver
Relative mRNA level
ZT2
ZT14
(b)
Dec1
Dec2
WT Co
WT HF
Dec1−/− Co
Dec1−/− HF

Figure 4

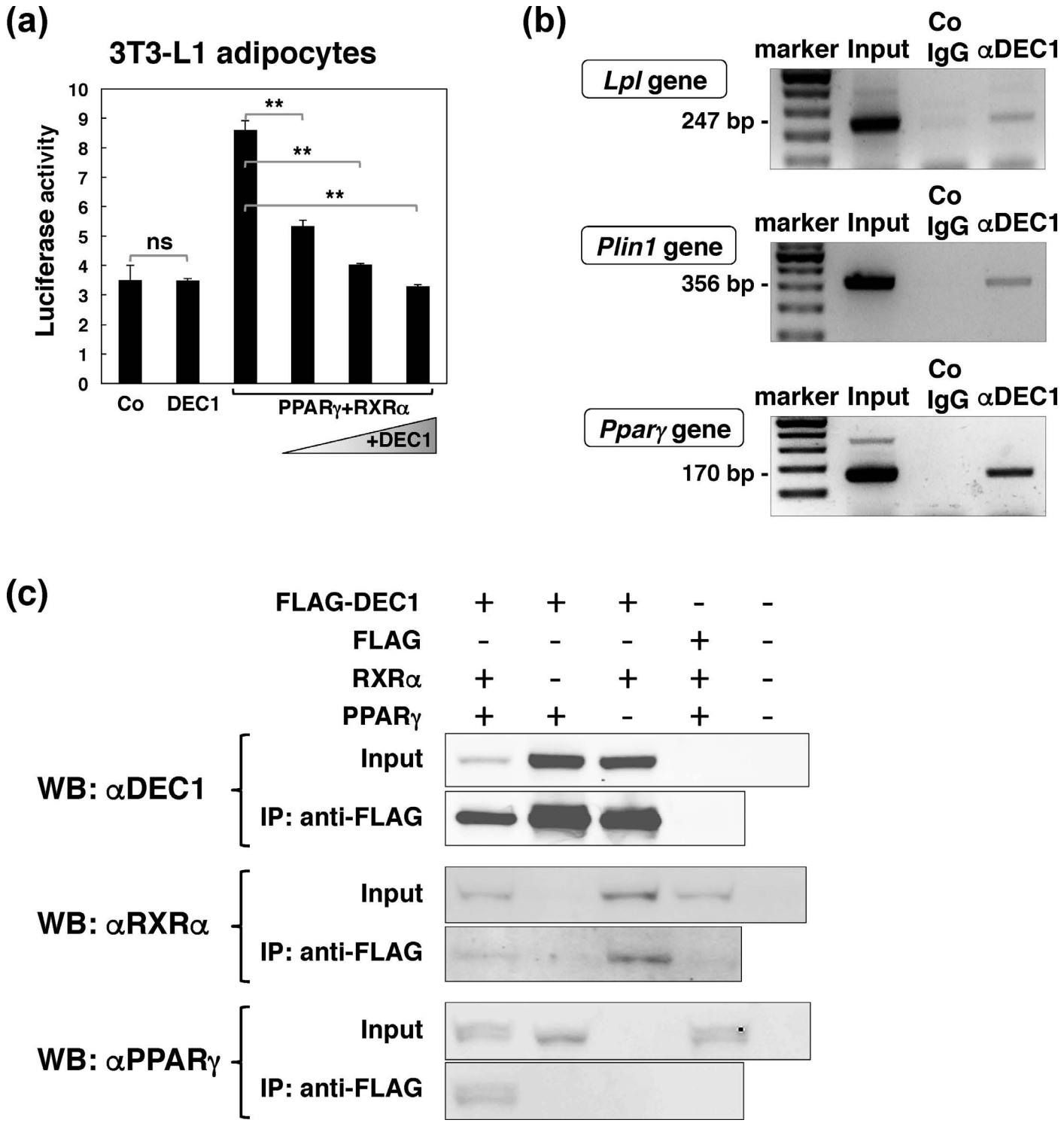
(a)
3T3-L1 adipocytes
Luciferase activity
10
9
8
7
6
5
4
3
2
1
0
**
**
**
ns
Co
DEC1
PPARγ+RXRα
+DEC1
(b)
marker
Input
Co IgG
αDEC1
Lpl gene
247 bp
Plin1 gene
356 bp
Pparγ gene
170 bp
(c)
FLAG-DEC1 + + + - -
FLAG - - - + -
RXRα + - + + -
PPARγ + + - + -
WB: αDEC1
Input
IP: anti-FLAG
WB: αRXRα
Input
IP: anti-FLAG
WB: αPPARγ
Input
IP: anti-FLAG

Figure 5

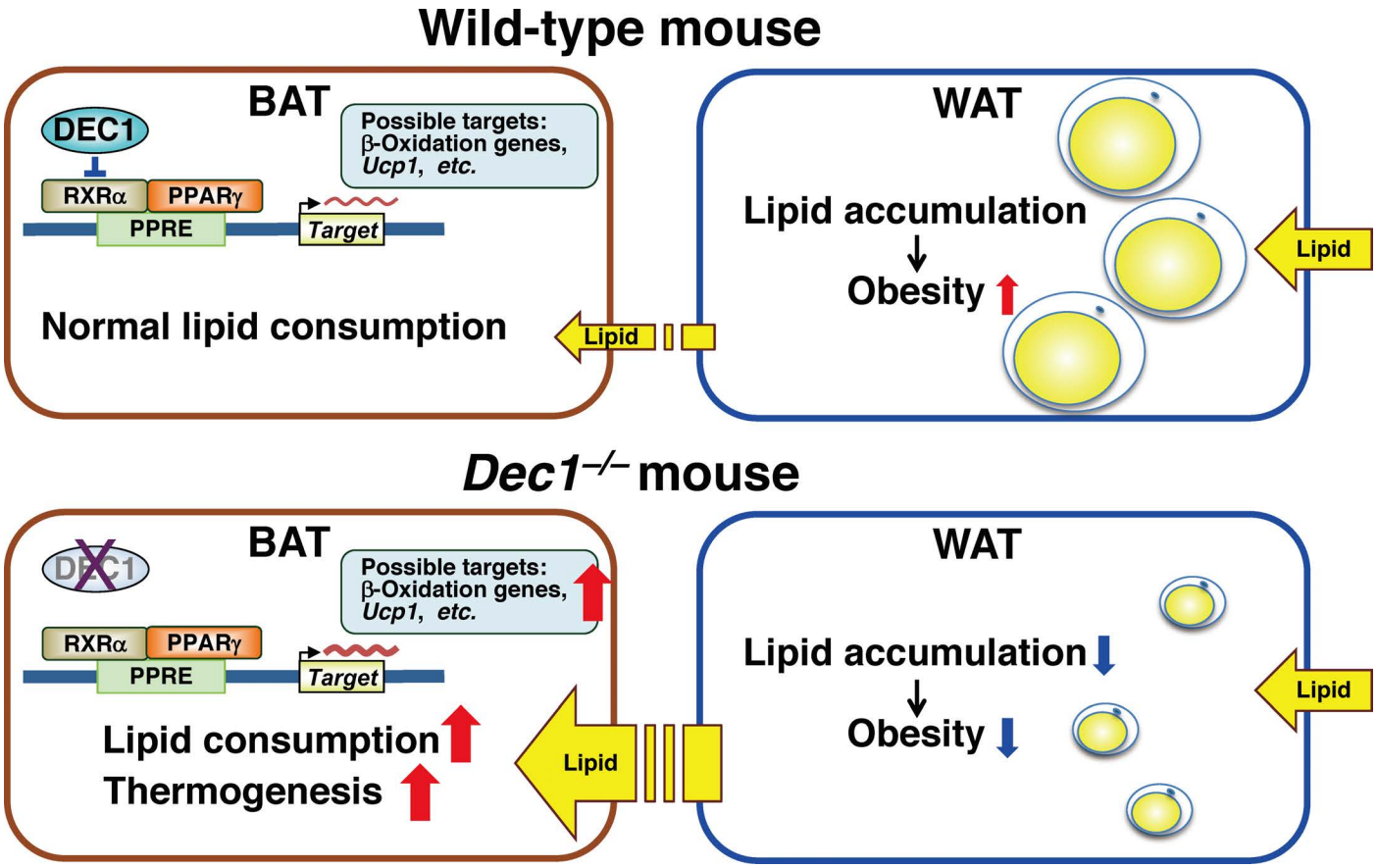
Wild-type mouse
BAT
DEC1
RXRα
PPARγ
PPRE
Target
Possible targets:
β-Oxidation genes,
Ucp1, etc.
Normal lipid consumption
Lipid
WAT
Lipid accumulation
Obesity
Lipid
Dec1−/− mouse
BAT
DEC1
RXRα
PPARγ
PPRE
Target
Possible targets:
β-Oxidation genes,
Ucp1, etc.
Lipid consumption
Thermogenesis
Lipid
WAT
Lipid accumulation
Obesity
Lipid